

## Article

# Impact Response of Composite Sandwich Cylindrical Shells

Paulo N. B. Reis <sup>1,\*</sup> , Carlos A. C. P. Coelho <sup>2</sup>  and Fábio V. P. Navalho <sup>2</sup><sup>1</sup> Department of Mechanical Engineering, CEMMPRE, University of Coimbra, 3030-788 Coimbra, Portugal<sup>2</sup> Escola Superior de Tecnologia de Abrantes, ESTA, Instituto Politécnico de Tomar, 2300-313 Tomar, Portugal; cccampos@ipt.pt (C.A.C.P.C.); fabionavalho@gmail.com (F.V.P.N.)

\* Correspondence: paulo.reis@dem.uc.pt

**Abstract:** Nowadays, due to the complexity and design of many advanced structures, cylindrical shells are starting to have numerous applications. Therefore, the main goal of this work is to study the effect of thickness and the benefits of a carbon composite sandwich cylindrical shell incorporating a cork core, compared to a conventional carbon composite cylindrical shell, in terms of the static and impact performances. For this purpose, static and impact tests were carried out with the samples freely supported on curved edges, while straight edges were bi-supported. A significant effect of the thickness on static properties and impact performance was observed. Compared to thinner shells, the failure load on the static tests increased by 237.9% and stiffness by 217.2% for thicker shells, while the restored energy obtained from the impact tests abruptly increased due to the collapse that occurred for the thinner ones. Regarding the sandwich shells, the incorporation of a cork core proved to be beneficial because it promoted an increase in the restored energy of around 44.8% relative to the conventional composite shell. Finally, when a carbon skin is replaced by a Kevlar one (hybridization effect), an improvement in the restored energy of about 20.8% was found. Therefore, it is possible to conclude that numerous industrial applications can benefit from cylindrical sandwiches incorporating cork, and their hybridization with Kevlar fibres should be especially considered when they are subject to impact loads. This optimized lay-up is suggested because Kevlar fibres fail through a series of small fibril failures, while carbon fibres exhibit a brittle collapse.

**Keywords:** composite sandwich cylindrical shells; low-velocity impact; experimental testingcheck for  
updates

**Citation:** Reis, P.N.B.; Coelho, C.A.C.P.; Navalho, F.V.P. Impact Response of Composite Sandwich Cylindrical Shells. *Appl. Sci.* **2021**, *11*, 10958. <https://doi.org/10.3390/app112210958>

Academic Editor: Ana Paula Betencourt Martins Amaro

Received: 17 October 2021  
Accepted: 12 November 2021  
Published: 19 November 2021

**Publisher's Note:** MDPI stays neutral with regard to jurisdictional claims in published maps and institutional affiliations.



**Copyright:** © 2021 by the authors. Licensee MDPI, Basel, Switzerland. This article is an open access article distributed under the terms and conditions of the Creative Commons Attribution (CC BY) license (<https://creativecommons.org/licenses/by/4.0/>).

## 1. Introduction

A high specific strength and stiffness, good static and dynamic properties, good corrosion resistance, adjustable properties, competitive cost, and fast manufacturing are factors that make composite materials very attractive in diverse fields of engineering. However, the weakness of these materials lies in their compression and transverse properties, which may even restrict their application. For example, their high sensitivity to low-velocity impacts, which can often occur in service or during maintenance activities, should be considered in the design phase because the resulting damage is difficult to detect [1,2] and, simultaneously, responsible for significant reductions in residual mechanical properties [3–6].

Regarding low-velocity impact events on through-thickness direction, the literature presents comprehensive knowledge at the level of damage mechanisms [7–10], residual compression after impact [11], multi-impacts [12] and environmental effects [13–15]. On the other hand, it is also possible to find strategies to improve the impact performance, for example, using hybridisation [16–18], nano-enhanced resins [19–23] or the inclusion of natural materials such as cork.

Cork is a natural and sustainable material, which presents excellent fire, smoke and toxicity properties associated with a high specific strength and stiffness, excellent damping characteristics, low thermal conductivity, near-zero Poisson coefficient, high damage tolerance to impact loads and resistance to wear [24–26]. At the level of benefits found in terms of impact, for example, Reis et al. [27] report improvements in terms of impact strength and

glass transition temperature when a polyester resin is filled with cork powder. Another study developed by the same authors shows benefits in terms of the elastic recuperation and damage area when an epoxy resin is filled with cork powder [21]. Simultaneously, the cork increased the penetration threshold and residual tensile strength [21]. Petit et al. [28] and Silva et al. [29] have also achieved significant benefits with the introduction of cork in composite laminates. For example, the latter observed a longitudinal crack and large delamination in monolithic laminates and when the cork layer was introduced, only a longitudinal crack was reported [29]. Amaro et al. [30] analysed the ballistic behaviour and damage tolerance of Kevlar/epoxy-reinforced composites with a matrix filled by cork powder and observed that the minimum velocity of perforation is similar, while there were fewer damaged areas when cork powder was added, in particular for velocities below the minimum perforation velocity. In terms of the residual bending strength, the authors found less sensitivity to impact velocity than samples with neat resin. In addition, cork powder reduces the amount of resin in the composite, making it more environmentally friendly. A similar benefit was observed by Reis et al. [31] in terms of fatigue strength where, regardless of the lower static bending strength, the fatigue life was not affected by adding cork powder into the resin. Finally, Ivañez et al. [32] studied the ballistic impact behaviour of monolithic laminates and composite sandwich plates incorporating a cork core. Low-velocity impact damage has previously been introduced to some laminates and sandwiches and subsequently subjected to ballistic impacts. No significant differences were observed between sandwich plates and laminates; however, the ballistic limit per area density of damaged laminates was reduced when compared to the value given for reference laminates, while in sandwich structures it was almost constant.

However, all these studies were carried out on composite plates, promoting, in this context, the consolidation of knowledge rather than what happens for composites cylindrical shells. In fact, there is not a lot of literature on the subject.

For example, Gong et al. [33] analytically studied the contact force and central deflection of a shell for different impact conditions, shell sizes and curvature values. This analytic solution included the contact deformation and transverse shear deformation, and a good agreement was found between their results and those in the literature. The impact response of cylindrical graphite/epoxy shells was analysed by Krishnamurthy et al. [34,35], and they found that higher impact energies (resulting from higher masses) promote longer contact times and more induced damage. An experimental study developed by Kistler [36] revealed that the impact response is very dependent on geometry. For example, stiffer structures have higher impact strength, less deflection and shorter contact time. Later, Kistler and Waas [37] developed studies in cylindrical graphite/epoxy panels with different thicknesses, curvatures, and boundary conditions. It was noticed that the peak impact force increased for higher thickness values, while the peak centre displacement and contact duration decreased. In fact, curvature effects have become increasingly important for smaller thicknesses. On the other hand, flatter panels had higher peak loads than curved panels, as well as smaller peak displacements and contact durations. With respect to boundary conditions, they found that changing from clamped to simply supported promote lower peak loads, while the peak displacement and contact duration increase. Zhao and Cho [38] analysed the effect of stacking sequence, radius of curvature and thickness on the impact energy threshold. The impact energy threshold is defined as the energy required to cause the initial impact damage. It was observed that the stacking sequence had a significant influence, because more interfaces between different plies can result in a higher impact velocity threshold and smaller damage size for the laminated shells. Regarding the radius of curvature, they observed that its decreasing promoted a higher impact velocity threshold and a smaller damage area. The maximum damage size increased as the shell became flatter because it became stiffer, and the position of the maximum damage area changed from the bottom interface ( $R = \infty$ ) to the top interface in the composite shells. Finally, larger thicknesses promoted smaller areas of damage because displacement is less prevalent in thicker shells. In fact, damage size is related to total dynamic deformation. Similar results

were found by Kumar [39], where a non-linear finite element analysis showed that the impact response is significantly dependent on the shell curvature. Finally, studies developed by Arachchige et al. [40,41] showed that the impact load increases with increasing stiffness, while the contact time decreases, and in relation to the impact velocity a direct relationship with the contact load was found. On the other hand, the hybridization effect was studied by Coelho et al. [42] and a strong effect was observed in terms of static and impact responses. For example, composites cylindrical shells involving only carbon fibres had the highest stiffness and the lowest displacement at maximum load, but with the introduction of the glass fibres and Kevlar fibres these configurations had, respectively, the lowest stiffness and the highest maximum load and displacement. Regarding the impact properties, composites cylindrical shells involving Kevlar fibres had the highest restored energy, while the non-hybrid ones had the lowest restored energy.

Therefore, the main goal of this work is to investigate the benefit of a composite sandwich cylindrical shell, incorporating a cork core, over a conventional composite cylindrical shell in terms of static and impact response. For this purpose, the results will be discussed based on the typical load versus displacement curves as well as load versus time and energy versus time curves. According to the authors' knowledge, there is still no study in the literature involving the benefits of cork in terms of composite cylindrical shells.

## 2. Material and Experimental Procedure

Composite cylindrical shells and composite sandwich cylindrical shells were produced by hand lay-up and the overall dimensions are shown in Figure 1. In detail, Figure 1a shows a view of the manufacturing process used in this study and Figure 1b the geometry and dimensions of the specimens.

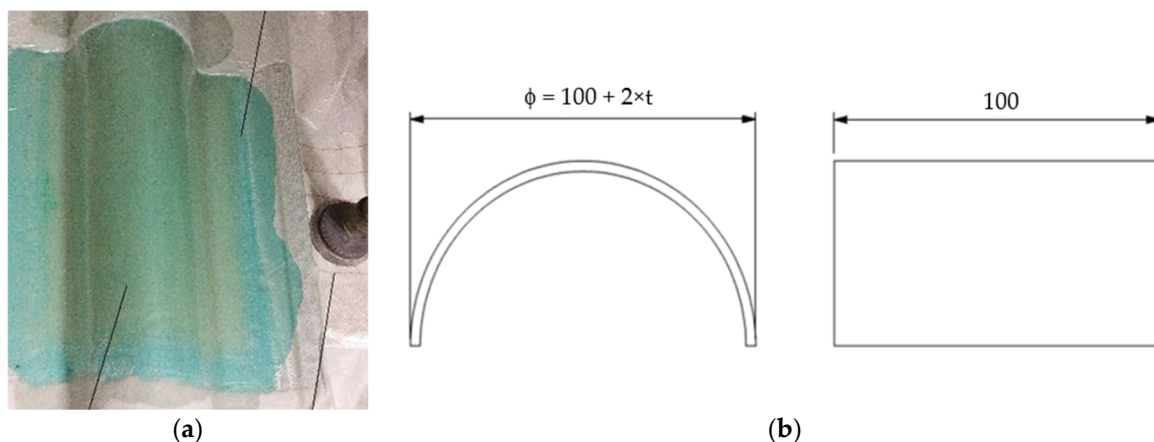


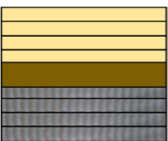
**Figure 1.** (a) Manufacturing process; (b) geometry and dimensions of the specimens in mm ( $t$  = thickness showed in Table 1).

A system of SR 1500 epoxy resin and a SD 2503 hardener standard, both supplied by Sicomin, was used as matrix and different number of layers and fibres, all in the same direction, were used to produce cylindrical shells with the following stacking sequences: 8C; 6C; 4C; 4C + cork + 4C and 4K + cork + 4C. The “number” represents the number of layers used, C = carbon bi-directional woven fabrics (taffeta with  $160 \text{ g/m}^2$ ), K = Kevlar bi-directional woven fabrics (taffeta with  $281 \text{ g/m}^2$ ) and cork is a 2 mm-thick NL 20 CORECORK layer (supplied by Amorim Cork Composites) inserted into the middle of the sheets. In detail, the carbon fibres used are of the T300 type, supplied by Toray, which have a density of  $1.76 \text{ g/cm}^3$  and a filament diameter of  $7 \text{ }\mu\text{m}$ , while for Kevlar fibres the density is  $1.44 \text{ g/cm}^3$  and the filament diameter is  $12 \text{ }\mu\text{m}$ , supplied by DuPont. The density of NL20 cork is  $0.25 \text{ g/cm}^3$ . These systems were placed inside a vacuum bag (see Figure 1a) for 24 h and a maximum vacuum pressure of 0.5 bar was applied for 9 h in order to maintain a constant fibre volume fraction and a uniform thickness to eliminate any

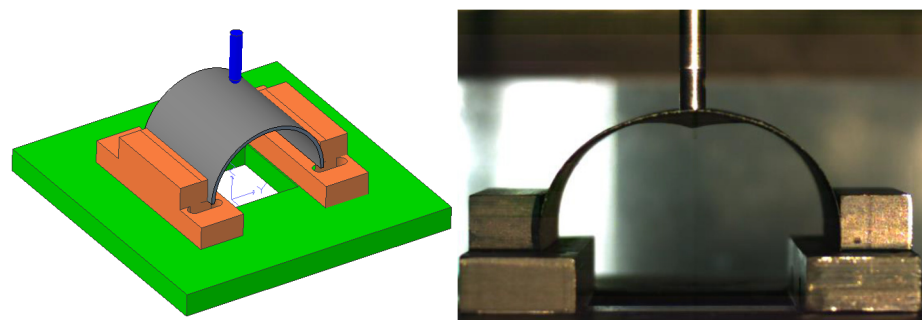
air bubbles existing in the laminate. According to the supplier's datasheet, the post-cure procedure was carried out in an oven at 60 °C for 16 h.

Table 1 summarizes the different thicknesses in terms of materials used and respective configurations.

**Table 1.** Stacking sequences and thicknesses of the samples tested.

| Stacking Sequence | Schematic Lay-Up   | Thickness (mm)<br>Average Value<br>(Standard Deviation) |
|-------------------|--|---|
| 8C                |    | 2.53 (0.15)   |
| 6C                |    | 1.58 (0.03)   |
| 4C                |    | 0.92 (0.02)   |
| 4C + Cork + 4C    |   | 4.23 (0.09)   |
| 4K + Cork + 4C    |  | 4.11 (0.03)   |

Static tests were carried out using a Shimadzu AG-100 universal testing machine, with the same support and loading nose used along the impact tests (Figure 2), equipped with a 100 kN load cell at a displacement rate of 3 mm/min. The displacement was obtained directly from the crosshead displacement that is automatically measured by the testing machine with a precision of  $\pm 0.01$  mm. These tests were carried out under conditions similar to those used in the impact tests, but, in this case, aiming to obtain the static characterization. All tests were carried out at room temperature, and five specimens were tested for each configuration.



**Figure 2.** Support used in the experimental tests.

Low-velocity impact tests were also performed using a drop weight testing machine IMATEK-IM10, and details of this impact machine can be found in [43]. An impactor diameter of 10 mm with a mass of 2.826 kg was used, which will impact the centre of the samples with free support on the curved edges while the straight edges are bi-supported

(Figure 2). An impact energy of 5 J was used, which was previously selected to promote visible damage, but without perforation of the specimens. The impact tests were performed in accordance with the considerations reported in ASTM D 7136 and, for each configuration, five specimens were tested at room temperature.

### 3. Results

Initially, the static properties were analysed and, for this purpose, bending tests were carried out for each configuration. Figure 3 shows the effect of thickness while Figure 4 shows the cork core effect and the hybridization effect in composite sandwich cylindrical shells. Typical load–displacement curves are shown, but they reflect the behaviour observed for each configuration.

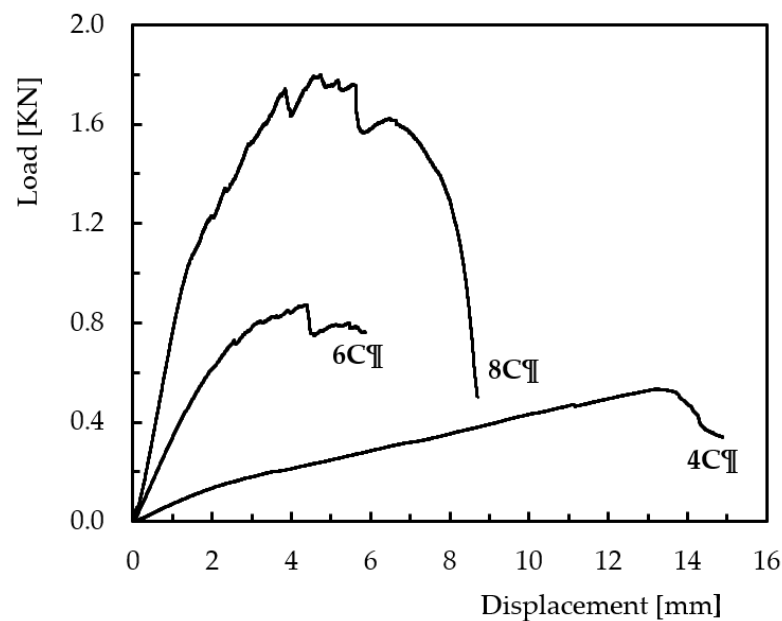


Figure 3. Effect of thickness on the compressive curves.

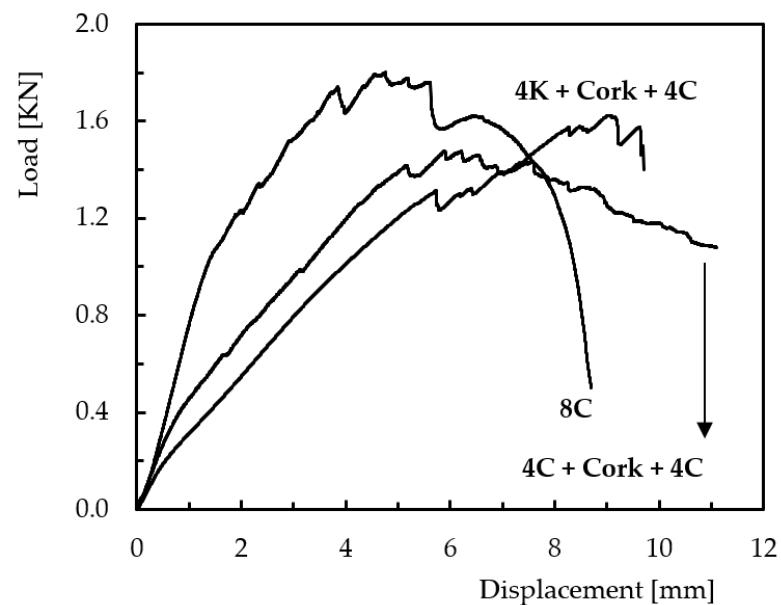


Figure 4. Cork core effect and hybridization effect on the compressive curves.

From the static curves related to the effect of thickness (Figure 3), it is possible to note for all materials a linear regime up to a value from which there is a non-linear regime that

contains the maximum load. However, increasing the thickness promotes longer linear regimes. For example, compared to cylindrical shells with four layers of carbon, where the linear regime goes up to a load around 120 N, this value is about 269% and 750% higher for cylindrical shells with 6 and 8 layers of carbon, respectively. The zigzag aspect of the curves results from fibre breakage and the subsequent drop in load is a consequence of the propagation of delaminations initiated at the regions with broken fibres, which is reported in the literature [5,6]. A similar behaviour is found when the cork core is introduced or for hybrid sandwich cylindrical shells but with different values. All properties that can be obtained from these curves are shown in Tables 2 and 3 in terms of average results and respective standard deviation. Stiffness was defined as the slope in the linear region of the load–displacement response and the displacement is the value obtained for the maximum load. The displacement, as reported above, was obtained directly from the crosshead displacement that is automatically measured by the testing machine.

**Table 2.** Effect of thickness on the compressive strength.

| Laminates | Maximum Load (N) |      | Displacement at Max. Load (mm) |      | Stiffness (N/mm) |      |
|-----------|------------------|------|--------------------------------|------|------------------|------|
|           | Average          | Std. | Average                        | Std. | Average          | Std. |
| 8C        | 1801             | 212  | 3.9                            | 0.7  | 812              | 29   |
| 6C        | 873              | 121  | 4.4                            | 1.0  | 354              | 41   |
| 4C        | 533              | 101  | 13.2                           | 2.1  | 71,7             | 8    |

**Table 3.** Cork core effect and hybridization effect on the compressive strength.

| Laminates      | Maximum Load (N) |      | Displacement at Max. Load (mm) |      | Stiffness (N/mm) |      |
|----------------|------------------|------|--------------------------------|------|------------------|------|
|                | Average          | Std. | Average                        | Std. | Average          | Std. |
| 8C             | 1801             | 212  | 4.7                            | 1.1  | 812              | 29   |
| 4C + Cork + 4C | 1476             | 121  | 5.9                            | 1.9  | 484              | 37   |
| 4K + Cork + 4C | 1623             | 101  | 9.1                            | 2.3  | 256              | 32   |

From Table 2, it is possible to observe a significant effect of the thickness on the bending properties, which agrees with the literature [44–46]. According to Ganapathi and Balamurugan [46], for example, an increase in the thickness of the shell reduces the instability region. From a quantitative point of view, and compared to thinner shells (4C), the load increases by 63.8% and 237.9% when the cylindrical shells are composed of 6 and 8 layers (6C and 8C), respectively. A similar trend was observed for stiffness, but with values of 393.7% and 1042.1%, respectively. On the other hand, in terms of displacement, as expected, this parameter decreases when the thickness increases. In this case, and compared to thicker cylindrical shells (8C), displacement at maximum load increases by around 12.8% and 238.5% for shells composed of 6 and 4 layers, respectively. In terms of damage mechanisms (see Figure 5), the failure analysis shows fibre fractures, which started in the fibres under compression, and some delaminations around the broken fibres. All these failure mechanisms arose in the indenter/composite contact region and agree with the literature [42,47], where the compressive stress concentration at the loading nose contact region associated with the low compressive strength of the fibres promotes the failure damage described above. For example, Figure 5a shows the failure mechanisms of the thicker shell, where the broken fibres are observed in the contact region of the indenter/composite and the consequent delaminations that result from this collapse. Subsequently, their propagation is visible along the generatrix that contains the contact point and towards the edge of the plate. However, because the stiffness is high, they do not reach the edge of the shell and fibre breakage occurs along the thickness (from the compression to the tensile side).

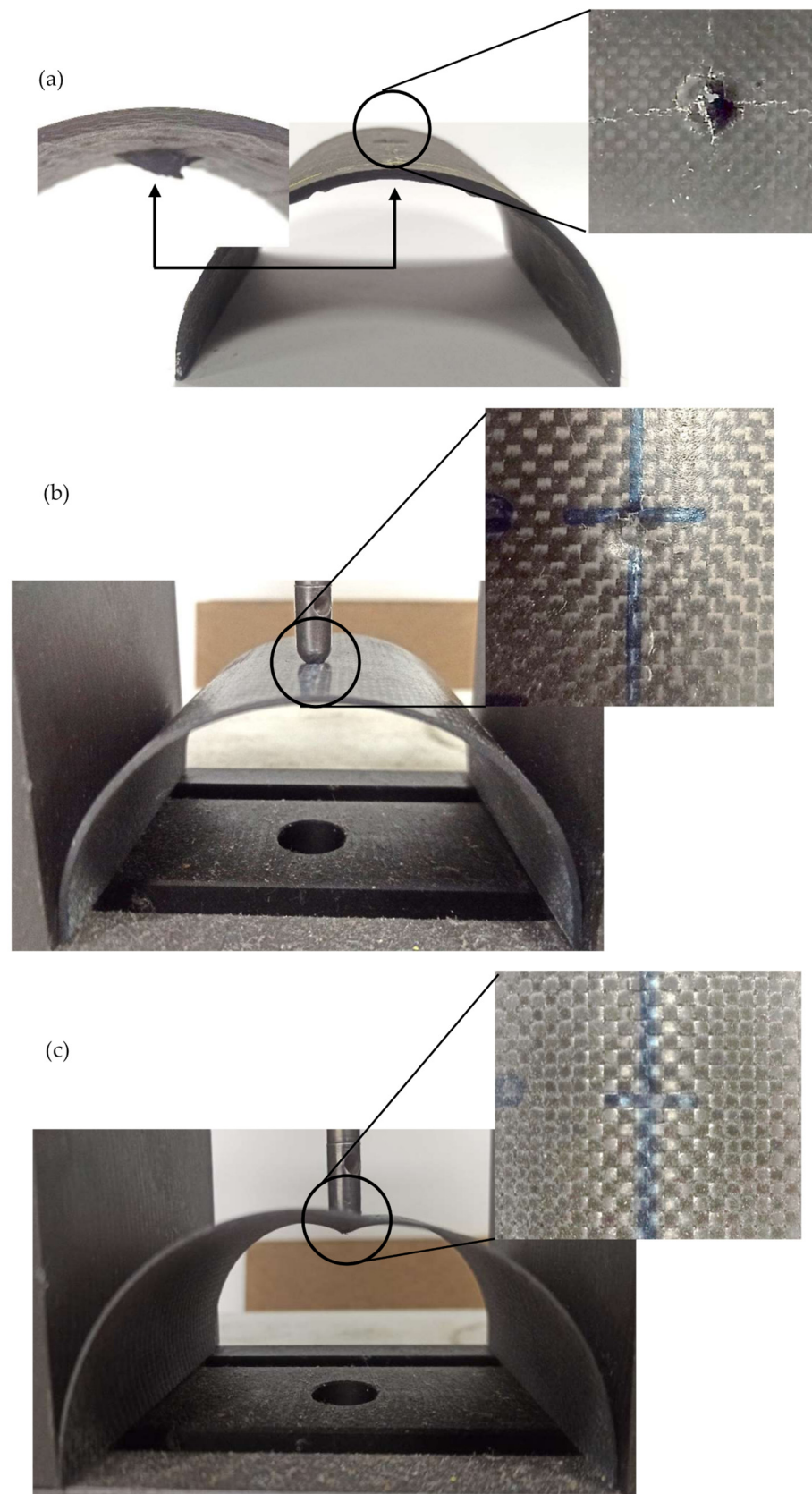


**Figure 5.** Failure mechanisms for shells with: (a) eight layers; (b) six layers; (c) four layers.

Regarding the shells with six layers of carbon fabric (Figure 5b), the damage mechanisms are similar, but due to the higher instability of the shell, the fibre breakage occur

essentially in the compression side and delaminations along the generatrix that contains the indenter/composite contact point is much longer than the previous ones (Figure 5a). Finally, for the thinner shells (Figure 5c), due to their enormous instability, it is possible to observe that the delaminations reach both edges and, in this case, some fibres break both in the compression and in the tensile side. Therefore, it is possible to conclude that the damages in thicker shells are more severe along the thickness, while in thinner ones the damages are more extensive.

On the other hand, from Table 3, it is possible to observe a significant effect of the cork core and the hybrid effect on the compressive properties. For example, compared to composite cylindrical shells (8C), when a cork layer is inserted into the middle of the shell (sandwich cylindrical shells), it promotes lower maximum loads and stiffness, while the displacement at maximum load increases. Decreases of around 18% and 40.4% can be found for maximum loads and stiffness, respectively, while the displacement at maximum load increases by about 25.5%. These values are in line with others reported in the literature [31,48–50], where the insertion of cork into composites decreases the bending strength and modulus, but the bending strain increases. In fact, cork deforms because the cell walls bend and buckle and can undergo large strain deformation. Therefore, the compression behaviour of cork is largely explained by the characteristics of its cellular structure [51]. However, other benefits are achieved, such as better impact performance [21,30,32,52]. In terms of damage mechanisms, Figure 6 shows the typical failure mechanism for the composite sandwich cylindrical shells, which are in line with those observed in Figure 5a. However, because the cork layer absorbs energy, the bottom face did not evidence any visible damage.

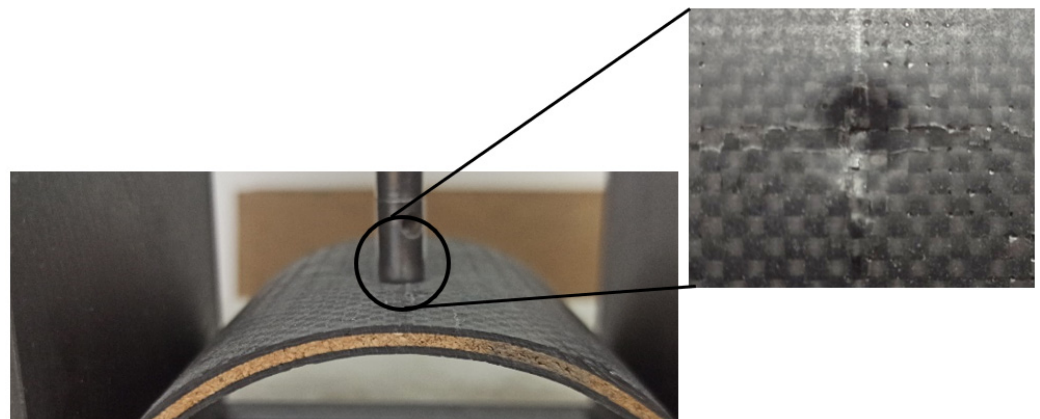


**Figure 6.** Failure mechanisms for composite sandwich cylindrical shells.

Concerning the hybridization, when a carbon skin is replaced by a Kevlar one, it is noticed that a higher maximum load and displacement are obtained, while the stiffness decreases. In this case, there were increases of about 10% and 54.2% for the maximum load and displacement, respectively, while the stiffness decreased by about 47.1%. According to Coelho et al. [42], regarding laminates with six layers, and comparing to cylindrical shells only with carbon fibres (6C), the maximum load is obtained for hybrid cylindrical shells involving carbon and Kevlar fibres, while the lowest value was obtained for those composed of carbon and glass fibres. In terms of stiffness, these authors observed that the highest value was obtained for cylindrical shells only with carbon fibres, while the lowest was obtained for hybrid shells of carbon and glass fibres. Finally, the smallest displacement occurred for cylindrical shells with carbon fibres and the largest value for the system involving carbon fibres and Kevlar. This behaviour was explained by the authors as result of the intrinsic mechanical properties of fibres and respective damage mechanisms. For example, while carbon fibre composites basically fail on the compression side, the glass fibre laminates fail on the tension side [53]. Therefore, when the carbon fibres are

placed on the tension side and glass fibres on the compressive side, an increase in flexural strength is obtained while the flexural modulus decreases [53,54]. However, these benefits depend on the fibre content, and according to the literature, the optimum value for hybrid carbon/glass composites is obtained for 12.5% of glass fibres placed on the compressive side [53,55].

In terms of impact response, Figure 7 shows the force–time and energy–time curves for composite cylindrical shells with different thicknesses (Figure 7a) and for composite sandwich cylindrical shells (Figure 7b).

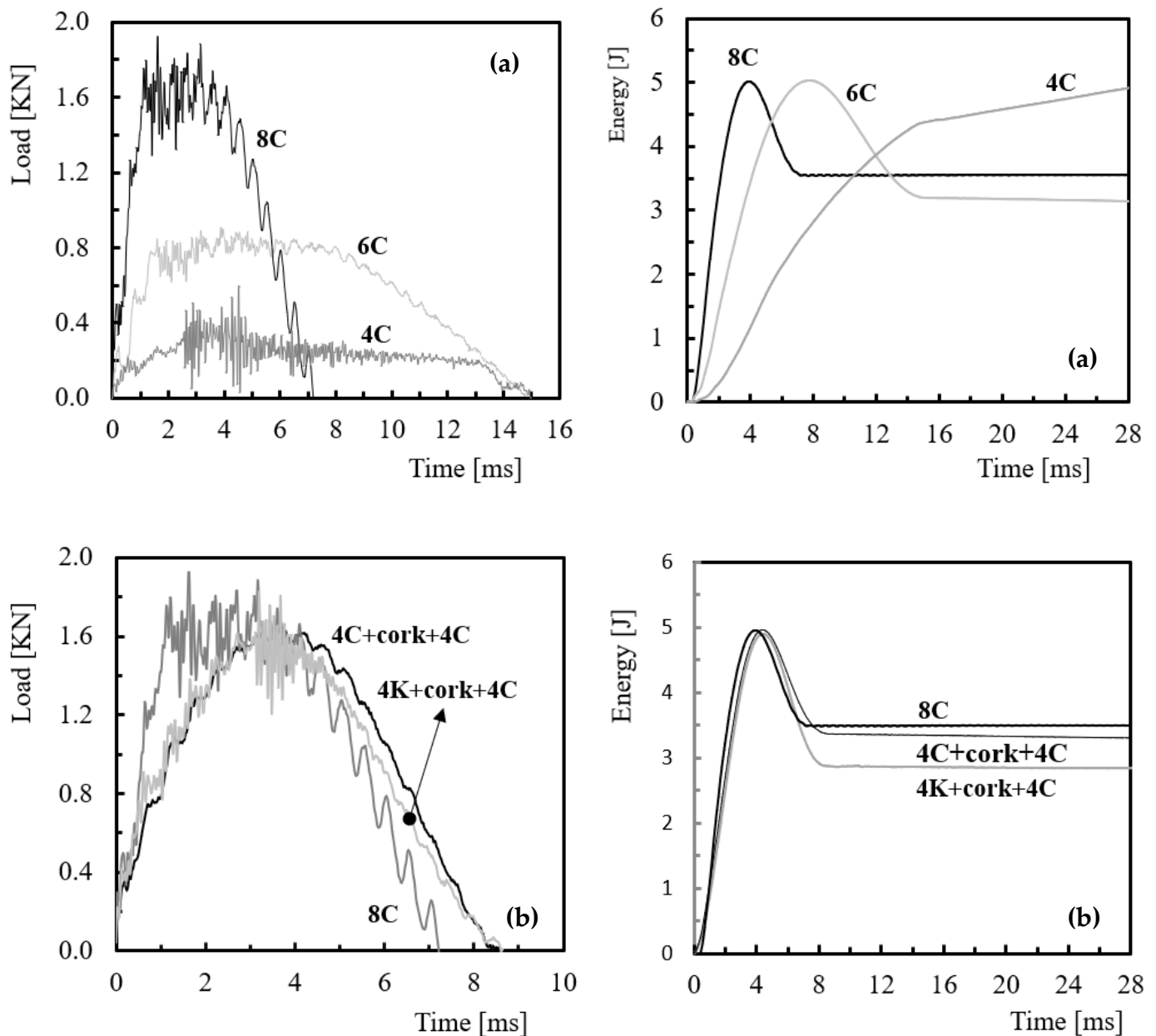


**Figure 7.** Load–time and energy–time curves for: (a) composite cylindrical shells with different thicknesses; (b) composite sandwich cylindrical shells.

These curves contain oscillations, which according to the literature [56,57], result from the elastic wave and are created by the vibrations of the samples. They are typical curves, representative of the other ones, and similar to those that can be found in the bibliography [19–21].

Regardless of the system tested, composite cylindrical shells or composite sandwich cylindrical shells, it is possible to observe that all load–time curves are characterized by an increase in the load up to a maximum value ( $P_{\max}$ ) followed by a drop after the peak load. However, for composite cylindrical shells with four layers (4C), after  $P_{\max}$  the load decreases and remains constant with increasing time. This atypical profile is a consequence of large damages, which can be proven through the energy–time curve where no energy is restored. Therefore, this means that the impact energy was mostly converted into damage. For the cylindrical shells with six layers (6C), the load–time curves behave similarly to the one described above. However, when it is analysed simultaneously with the energy–time curve, it is possible to conclude that despite the high damage introduced into the shell there is still a significant amount of restored energy (around 34.2% of the impact energy). Finally, for the cylindrical shells with eight layers (8C), the load–time curves present the typical behaviour reported in the literature [19–21]. Nevertheless, when the energy–time curve is compared with the others, it is possible to observe that this configuration absorbs more energy than, for example, the configuration with six layers (about 11.3% more). In this case, this higher amount of energy absorbed is reflected in larger internal damages. Figure 8, for example, shows the failure surface for the various configurations.

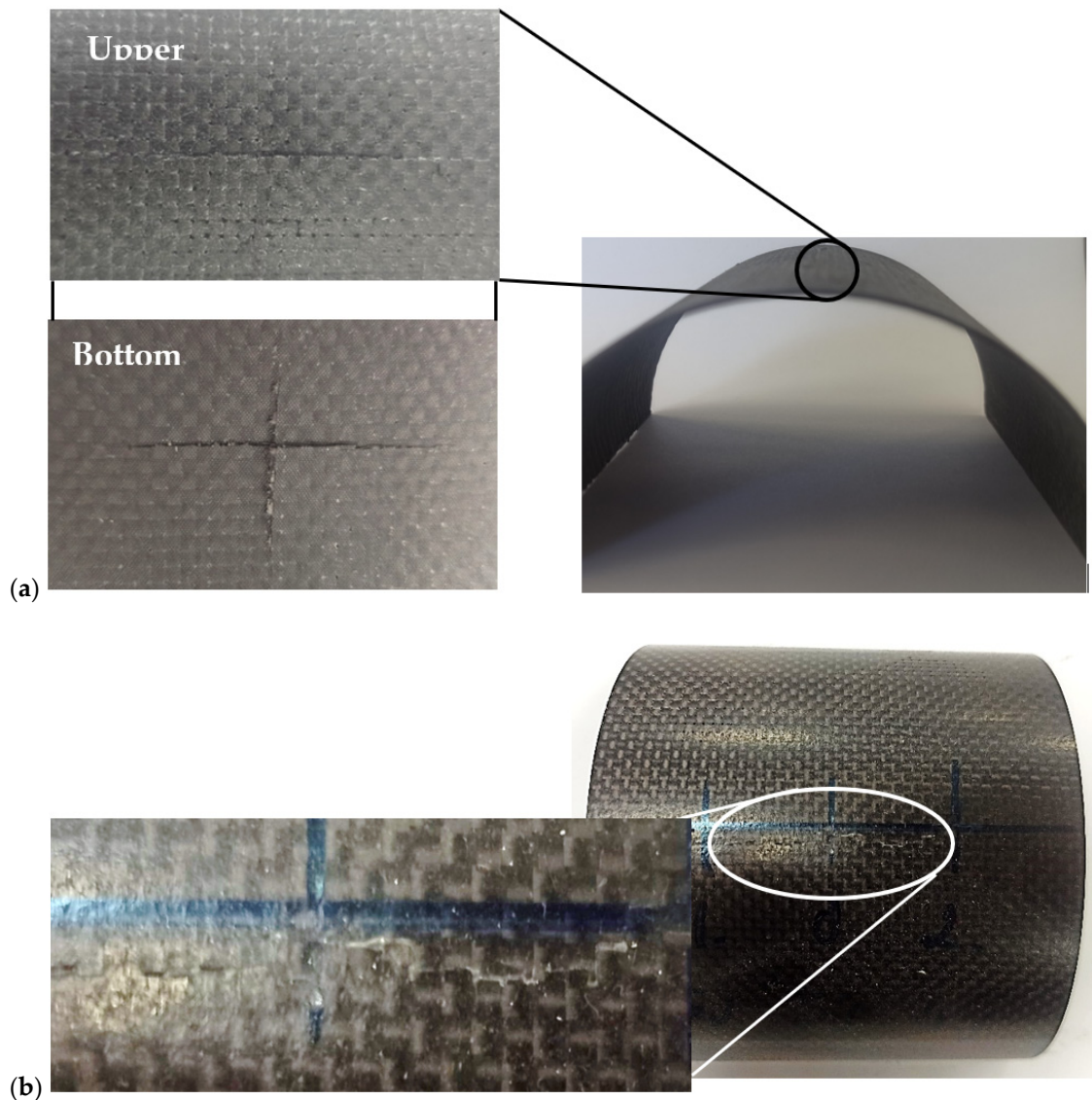
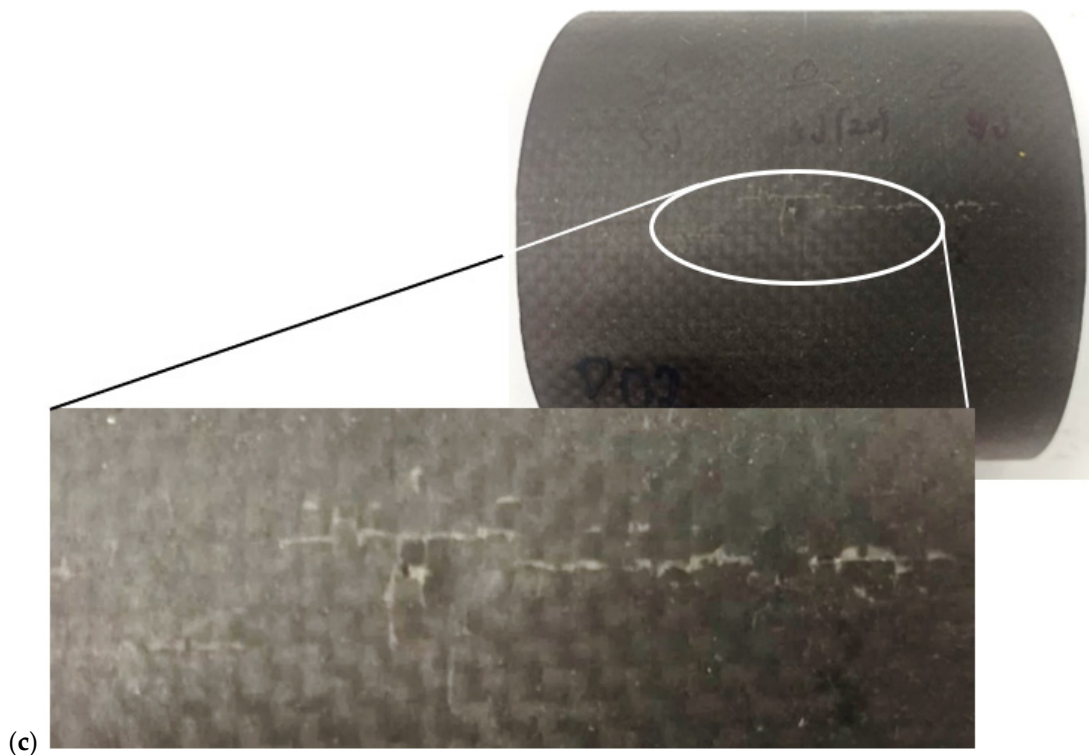


Figure 8. Cont.



**Figure 8.** Failure mechanisms after impact for shells with: (a) four layers; (b) six layers; (c) eight layers.

From Figure 8, it is possible to notice that for the thinner shells (Figure 8a), the damage starts in the impactor/composite contact zone, in the form of fibre breakage and delaminations around them. There is even full perforation of the shell along its thickness. Regarding the six-layer shells (Figure 8b), damage also starts in the impact zone with fibre breakage, but only on the compression side, and delaminations around the broken fibres that have propagated towards the edge. Although the damage is visible to the naked eye, there was no perforation of the shells due to their greater stiffness. Finally, for thicker shells (Figure 8c), the damage is more localized due to a higher thickness, and the indications expressed in Figure 8c show that it develops more along the thickness in form of delaminations. In this case, thickness is an important parameter both in static and impact strength. In fact, according to Zhao and Cho [38], higher thicknesses promote smaller areas of damage because displacement is less in thicker shells, and the damage size is related to total dynamic deformation. Compared to the flat plates, the damage size becomes smaller and its position changes from the lower interface to the upper interface in composite shells [38]. Therefore, the damage appears first at the top ply and then propagates to the bottom layers; however, the maximum damage area occurs at the top surface [38]. In addition, it should also be taken into account that the severity of the damage is higher because carbon fibres fail mainly on the compression side in composites exposed to bending mode [53]. On the other hand, studies developed by Kistler [36] revealed that stiffer structures have a higher impact strength, less deflection and shorter contact times.

According to the literature [21], the value of  $P_{max}$  is very important because it depends on the impact energy and represents the peak load value that the composite can tolerate, under a particular impact level, before undergoing major damage. Therefore, Table 4 presents the average values, and respective standard deviation, of the peak load and other parameters (maximum displacement and rebounded energy (elastic recuperation)) obtained from the impact tests. The elastic recuperation is the difference between the absorbed energy and the energy at peak load [19]. From the results, it is possible to observe that all properties are very dependent on thickness, reproducing the same effect found for static properties.

**Table 4.** Average values of the peak load, maximum displacement and elastic recuperation for composite cylindrical shells.

| Laminates | Peak Load (N) |      | Max Displacement (mm) |      | Elastic Recuperation (J) |      |
|-----------|---------------|------|-----------------------|------|--------------------------|------|
|           | Average       | Std. | Average               | Std. | Average                  | Std. |
| 8C        | 1959          | 50   | 4.2                   | 0.02 | 1.16                     | 0.38 |
| 6C        | 924           | 12   | 7.8                   | 0.19 | 1.71                     | 0.19 |
| 4C        | 589           | 4    | -                     | -    | -                        | -    |

In terms of maximum load ( $P_{\max}$ ), this value increases with increasing thickness, reaching an increase of 232.6% for the analysed shells (between 4C and 8C). On the other hand, the displacement decreases by around 46.2% between shells with six and eight layers, while for shells with four layers of carbon fabric the collapse was observed (no restored energy). This behaviour agrees with the studies developed by Kistler and Waas [37] and Arachchige et al. [40,41], where it was observed that the peak impact load increased with increasing thickness, while the peak centre displacement and contact duration decreased. Amaro et al. [58] observed that the maximum load increased with the thickness of the plate, while the displacement decreased, due to delaminations that proved to be the main mode of damage. They found that higher thicknesses were responsible for larger delaminations.

Regarding the elastic recuperation, a decrease of around 32.2% was found between shells with six and eight layers, while for composite shells with four layers of carbon fabric no restored energy was observed. As described above, although visible damage is more severe in shells with six layers of carbon (6C), the energy absorbed is less than in thicker shells (8C). In fact, the maximum damage area occurs at the top surface and propagates to the bottom [38], but smaller areas are expected with increasing thickness due to smaller displacements. However, although the damage at the top surface is less, it propagates along the thickness, promoting, in this case, delaminations capable of absorbing impact energy. According to the literature [59], during an impact event, the energy is absorbed by matrix cracking, delamination and fibre breakage, but most of it is absorbed essentially by deflection and delaminations. Nevertheless, because the deflection is lower due to the greater thickness of the shell, and consequent higher stiffness, it is expected that there will be a greater density of delaminations to absorb the same impact energy. On the other hand, smaller thicknesses promote greater deflections and, consequently, lower delamination density [58].

In fact, according to García-Castillo et al. [60], thickness is one of the main parameters that determine the impact properties, in particular the perforation velocity or the perforation-threshold energy. However, as an alternative parameter, the literature suggests the areal density (mass per unit area), which has been studied by several authors [61–64]. A non-linear relationship between perforation-threshold energy and thickness was even proposed by Grujicic et al. [64]. Zhu et al. [65], for example, found that the perforation velocity varies linearly with the laminate thickness within the range of 3 to 14 mm, while He et al. [66] noticed a non-linear relationship for a wide range of thicknesses below 16 mm.

Taking in account these studies, and considering the values shown in Table 4, the maximum load ( $P_{\max}$ ) is plotted against the areal density in Figure 9. It is possible to observe a non-linear relationship between maximum load and areal density (thickness), which is in good agreement with the studies developed by Grujicic et al. [64], although the considered impact parameter by these authors is different (perforation-threshold energy). Considering only the six (6C) and eight (8C) layers of carbon, the absorbed energy per areal density is around  $1.42 \text{ J/kg}\cdot\text{m}^{-2}$  and  $1.08 \text{ J/kg}\cdot\text{m}^{-2}$ , respectively. These results evidence that the effect of the thickness on the impact properties is determinant, because, while the absorbed energy increased by around 17%, the areal density increased about 53%.

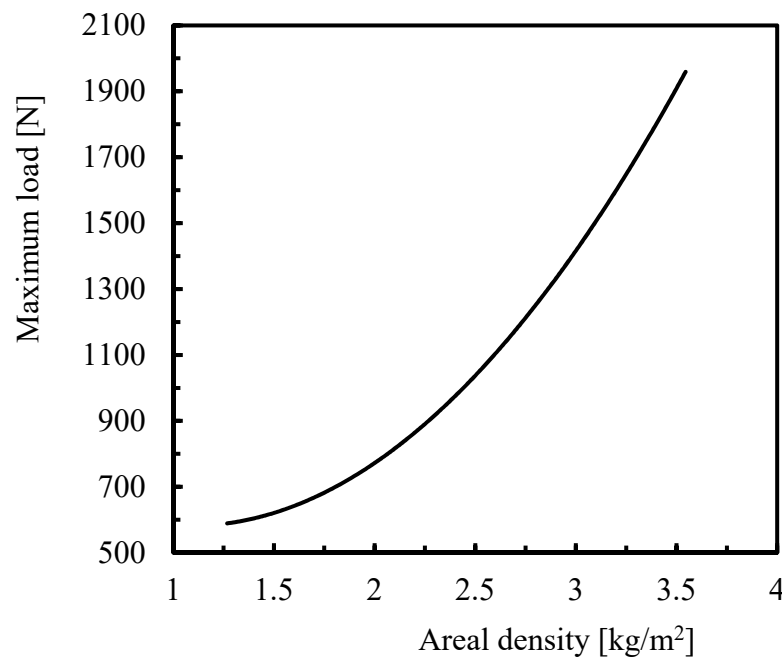


**Figure 9.** Maximum load versus areal density.

When composite sandwich cylindrical shells are compared, in terms of impact response, to conventional composite cylindrical shells (Figure 7b), the load–time curves are very similar, showing only a longer contact time for the sandwich shells. In terms of elastic recuperation, the benefits of introducing the cork layer are evident due to the intrinsic properties of this material. Cork has a high damage tolerance to impact loads [24–26] because under compressive loading (during the impact) the cell walls bend and buckle, promoting, in this case, a large deformation. This explains the larger displacements and lower maximum loads observed in shells that incorporate a cork layer. Simultaneously, when the cell walls bend and buckle, they absorb significant amounts of energy with a high viscoelastic return. Therefore, after each impact, cork continues to have the ability to absorb energy, which does not change due to its elastic deformation [51,67]. This evidence is quantified in Table 5 in terms of mean values and respective standard deviations, for peak load, maximum displacement and bounced energy (elastic recovery). For example, compared to the conventional shells (8C), the maximum impact load decreased by around 10.4% when the cork layer was inserted into the middle of the shell, while the maximum displacement increased about 11.9%. In terms of elastic recuperation an increase of around 44.8% is observed. In addition to the reported benefits, cork is also responsible for increasing the impact threshold when inserted into polymeric composites [21,52]. Studies developed by Reis et al. [21] and Silva et al. [52] showed, for example, benefits of around 9% to 12.6% in relation to laminates without cork (neat resin).

**Table 5.** Average values of the peak load, maximum displacement and elastic recuperation for composite sandwich shells.

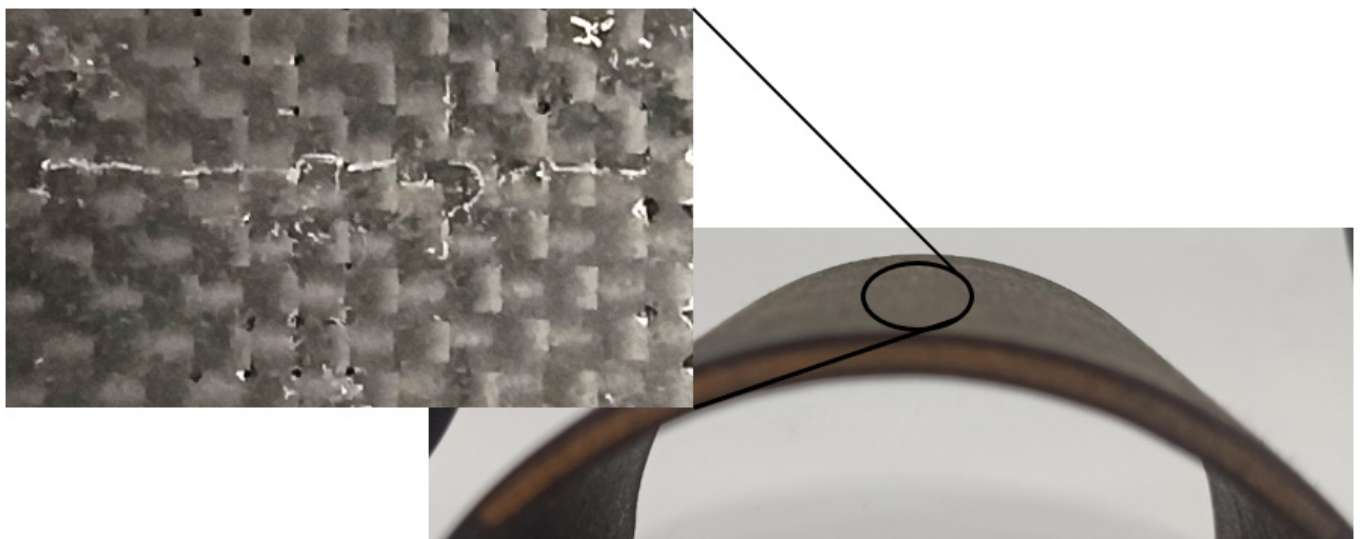
| Laminates      | Peak Load [N] |      | Max Displacement [mm] |      | Elastic Recuperation [J] |      |
|----------------|---------------|------|-----------------------|------|--------------------------|------|
|                | Average       | Std. | Average               | Std. | Average                  | Std. |
| 8C             | 1959          | 50   | 4.2                   | 0.02 | 1.16                     | 0.38 |
| 4C + Cork + 4C | 1755          | 92   | 4.7                   | 0.05 | 1.68                     | 0.01 |
| 4K + Cork + 4C | 1653          | 21   | 4.9                   | 0.13 | 2.03                     | 0.01 |

However, in relation to the benefits obtained with the hybridization of composite sandwich shells, from Table 5 it is possible to observe, compared to sandwiches shells with carbon alone, lower peak loads and higher maximum displacements, as well as elastic

recuperation (restored energy). For example, the maximum impact load (peak load) is 5.8% lower, while the maximum displacement and restored energy are about 4.3% and 20.8% higher, respectively. In this case, the hybridization further improved the impact performance of the sandwiches with the incorporation of aramid fibres (Kevlar), which agrees with studies developed by Coelho et al. [42]. According to these authors, composites' cylindrical shells incorporating Kevlar fibres showed the highest restored energy, while the non-hybrid ones (6C) had the lowest restored energy, in addition to lower maximum impact load and higher displacements. It was observed by the authors that, as a consequence of higher damages, the restored energy of the carbon shells (1.71 J) was the lowest, while the hybrid configuration involving carbon and Kevlar fibres (2C + 2K + 2C) showed a much higher elastic recuperation (37.4% higher). This shows that stiffer structures (see Table 3) produce higher impact forces, smaller deflections, and shorter contact duration times [36,37,39]. Consequently, an optimization process in design is suggested because the minimum damage zone is achieved for equal bending stiffnesses in both the axial and circumferential directions [38]. In fact, aramid fibres fail not through brittle cracks like carbon fibres, but through a series of small fibril failures, where the fibrils are molecular strands that make up each aramid fibre and are oriented in the same direction as the fibre itself. These small failures absorb a large amount of energy, leading to a very high tenacity.

Finally, the failure surface observed after impact for sandwich shells is shown in Figure 10, where it is possible to observe some similarity with the surfaces obtained in the static tests. In both sandwiches, the damage is very confined to the impactor/composite contact zone.

For sandwiches involving only carbon fibres, fibre breakage occurs on the compression side due to the low compressive strength of these fibres, and around them some delaminations occur. Regarding the hybrid sandwiches, the damage mechanism is very similar but much more confined to the impactor/composite contact zone. As mentioned above, the damage appears at the top ply and propagates to the bottom layers but, due to the cork core, it is expected that it stops at the composite/cork interface and promotes large delaminations in this region.



(a)

Figure 10. Cont.

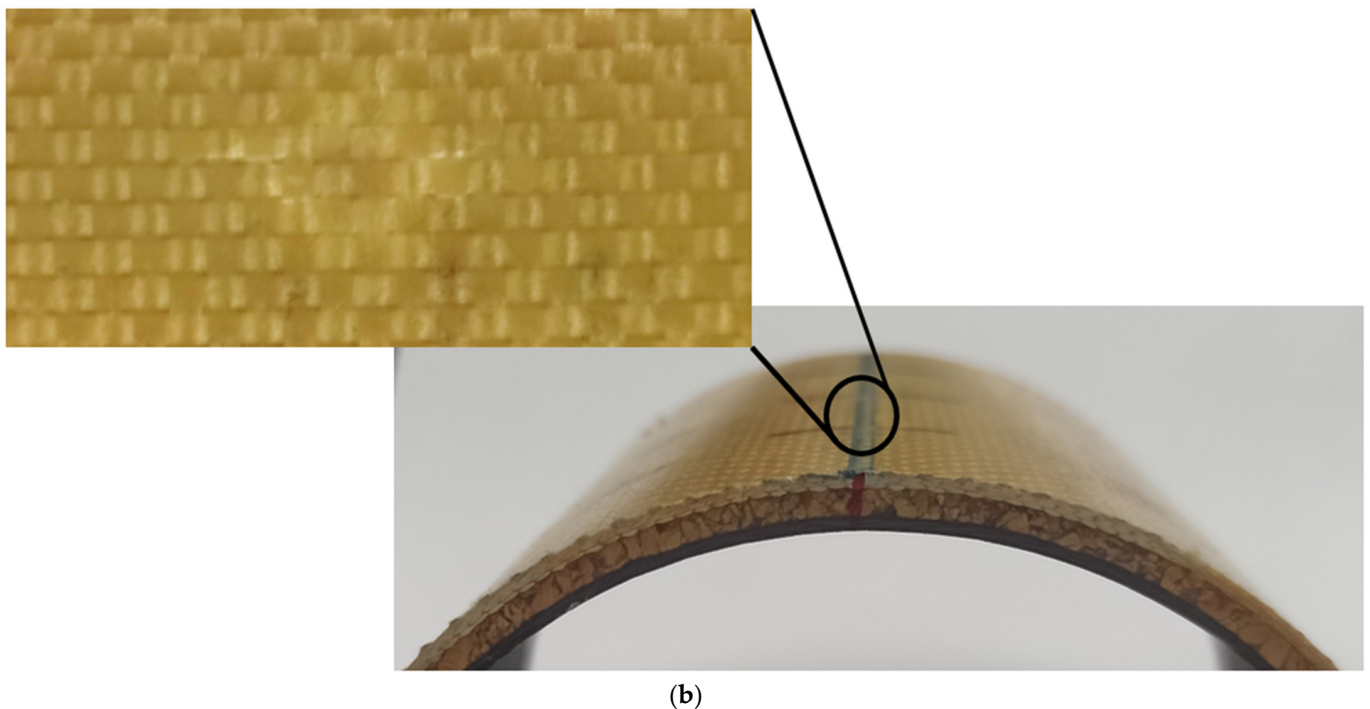


**Figure 10.** Failure mechanisms after impact for: (a) carbon sandwich shells; (b) hybrid sandwich shells.

#### 4. Conclusions

This work studied the effect of thickness on a carbon composite sandwich cylindrical shell and the benefits of a carbon composite sandwich cylindrical shell incorporating a cork core, compared to a conventional carbon composite cylindrical shell. Static bending tests and low-velocity impact tests were performed on specimens that were freely supported on the curved edges, while the straight edges were bi-supported.

In terms of static bending properties, it was possible to find a significant effect of the thickness. For example, compared to thinner shells (4C), thicker shells (8C) have higher peak load and stiffness values of about 237.9% and 2149.3%, respectively, while the displacement at maximum load decreased 70.5%. Regarding the carbon composite sandwich cylindrical shells incorporating cork core, decreases of around 18% and 40.4% were found for the maximum load and stiffness, respectively, while the displacement at maximum load increases about 25.5%. These benefits were explained by the intrinsic properties of the cork. However, when the sandwich shell was hybridized with Kevlar fibres, higher maximum loads (10%) and displacements (54.2%) were obtained, while the stiffness decreased (47.1%) compared to the conventional carbon composite cylindrical shell.

Finally, in terms of impact performance, it was observed that larger thicknesses promote significant improvements in the restored energy because, for example, the perforation was observed for the thinner shells (4C). For composite sandwich shells, improvements in impact strength were obtained when a cork layer was introduced, but they were further increased when a carbon skin was replaced by a Kevlar one (hybridization effect). For example, compared to the conventional carbon shell, when a cork layer was inserted into the carbon shell, it allowed the maximum load to be decreased, but increased the maximum displacement and the restored energy. This trend was further evidenced with the replacement of a carbon skin by Kevlar fibres. Comparing the elastic recuperation, for example, improvements of around 44.8% and 20.8% were found, respectively.

Therefore, this study allows us to conclude that numerous industrial applications that use cylindrical sandwiches can benefit from the use of a cork core and the face that is eventually subject to impact loads should incorporate Kevlar fibres to increase the sandwich's impact strength. This optimized lay-up is suggested because these fibres fail through a series of small fibril failures, while carbon fibres exhibit a brittle collapse.

**Author Contributions:** C.A.C.P.C. analysed the results and helped to write the manuscript; F.V.P.N. performed the impact test and produced the laminates; P.N.B.R. analysed the results and helped to write the manuscript. All authors have read and agreed to the published version of the manuscript.

**Funding:** This research received no external funding.

**Institutional Review Board Statement:** Not applicable.

**Informed Consent Statement:** Not applicable.

**Data Availability Statement:** Not applicable.

**Acknowledgments:** This research is sponsored by national funds through FCT—Fundação para a Ciência e a Tecnologia, under the project UIDB/00285/2020.

**Conflicts of Interest:** The authors declare no conflict of interest.

## References

1. Adams, R.D.; Cawley, P.D.R.D. A review of defects types and non-destructive testing techniques for composites and bonded joints. *NDT E Int.* **1998**, *21*, 208–222. [\[CrossRef\]](#)
2. Amaro, A.M.; Reis, P.N.B.; de Moura, M.F.S.F.; Santos, J.B. Damage detection on laminated composite materials using several NDT techniques. *Insight* **2012**, *54*, 14–20. [\[CrossRef\]](#)
3. De Moura, M.F.S.F.; Marques, A.T. Prediction of low velocity impact damage in carbon-epoxy laminates. *Compos. Part A Appl. Sci.* **2002**, *33*, 361–368. [\[CrossRef\]](#)
4. Reis, P.N.B.; Ferreira, J.A.M.; Antunes, F.V.; Richardson, M.O.W. Effect of interlayer delamination on mechanical behavior of carbon/epoxy laminates. *J. Compos. Mater.* **2009**, *43*, 2609–2621. [\[CrossRef\]](#)
5. Amaro, A.M.; de Moura, M.F.S.F.; Reis, P.N.B. Residual strength after low velocity impact in carbon-epoxy laminates. *Mater. Sci. Forum* **2006**, *514–516*, 624–628. [\[CrossRef\]](#)
6. Amaro, A.M.; Reis, P.N.B.; de Moura, M.F.S.F. Delamination effect on bending behaviour in carbon-epoxy composites. *Strain* **2011**, *47*, 203–208. [\[CrossRef\]](#)
7. Richardson, M.O.W.; Wisheart, M.J. Review of low-velocity impact properties of composite materials. *Compos. Part A Appl. Sci.* **1996**, *27*, 1123–1131. [\[CrossRef\]](#)
8. Río, T.G.; Zaera, R.; Barbero, E.; Navarro, C. Damage in CFRPs due to low velocity impact at low temperature. *Compos. Part B Eng.* **2005**, *36*, 41–50. [\[CrossRef\]](#)
9. Aktas, M.; Atas, C.; Icten, B.M.; Karakuzu, R. An experimental investigation of the impact response of composite laminates. *Compos. Struct.* **2009**, *87*, 307–313. [\[CrossRef\]](#)
10. Dhakal, H.N.; Zhang, Z.Y.; Bennett, N.; Reis, P.N.B. Low-velocity impact response of nonwoven hemp fibre reinforced unsaturated polyester composites: Influence of impactor geometry and impact velocity. *Compos. Struct.* **2012**, *94*, 2756–2763. [\[CrossRef\]](#)
11. Kulkarni, M.D.; Goel, R.; Naik, N.K. Effect of back pressure on impact and compression after-impact characteristics of composites. *Compos. Struct.* **2011**, *93*, 944–951. [\[CrossRef\]](#)
12. Amaro, A.M.; Reis, P.N.B.; de Moura, M.F.S.F.; Neto, M.A. Influence of multi-impacts on GFRP composites laminates. *Compos. Part B Eng.* **2013**, *52*, 93–99. [\[CrossRef\]](#)
13. Amaro, A.M.; Reis, P.N.B.; Neto, M.A.; Louro, C. Effects of alkaline and acid solutions on glass/epoxy composites. *Polym. Degrad. Stabil.* **2013**, *98*, 853–862. [\[CrossRef\]](#)
14. Mortas, N.; Er, O.; Reis, P.N.B.; Ferreira, J.A.M. Effect of corrosive solutions on composites laminates subjected to low velocity impact loading. *Compos. Struct.* **2014**, *108*, 205–211. [\[CrossRef\]](#)
15. Amaro, A.M.; Reis, P.N.B.; Neto, M.A. Experimental study of temperature effects on composite laminates subjected to multi-impacts. *Compos. Part B Eng.* **2016**, *98*, 23–29. [\[CrossRef\]](#)
16. Hosur, M.V.; Adbullah, M.; Jeelani, S. Studies on the low-velocity impact response of woven hybrid composites. *Compos. Struct.* **2005**, *67*, 253–262. [\[CrossRef\]](#)
17. Halvorsen, A.; Salehi-Khojin, A.; Mahinfalah, M.; Nakhaei-Jazar, R. Temperature effects on the impact behavior of fiberglass and fiberglass/Kevlar sandwich composites. *Appl. Compos. Mater.* **2006**, *13*, 369–383. [\[CrossRef\]](#)
18. Salehi-Khojin, A.; Mahinfalaha, M.; Bashirzadeh, R.; Freeman, B. Temperature effects on Kevlar/hybrid and carbon fiber composite sandwiches under impact loading. *Compos. Struct.* **2007**, *78*, 197–206. [\[CrossRef\]](#)
19. Ávila, A.F.; Soares, M.I.; Neto, A.S. A study on nanostructured laminated plates behavior under low-velocity impact loadings. *Int. J. Impact Eng.* **2007**, *34*, 28–41. [\[CrossRef\]](#)
20. Iqbal, K.; Khan, S.-U.; Munir, A.; Kim, J.-K. Impact damage resistance of CFRP with nanoclay-filled epoxy matrix. *Compos. Sci. Technol.* **2009**, *69*, 1949–1957. [\[CrossRef\]](#)
21. Reis, P.N.B.; Ferreira, J.A.M.; Santos, P.; Richardson, M.O.W.; Santos, J.B. Impact response of Kevlar composites with filled epoxy matrix. *Compos. Struct.* **2012**, *94*, 3520–3528. [\[CrossRef\]](#)
22. Reis, P.N.B.; Ferreira, J.A.M.; Zhang, Z.Y.; Benameur, T.; Richardson, M.O.W. Impact response of Kevlar composites with nanoclay enhanced epoxy matrix. *Compos. Part B Eng.* **2013**, *46*, 7–14. [\[CrossRef\]](#)

23. Reis, P.N.B.; Ferreira, J.A.M.; Zhang, Z.Y.; Benameur, T.; Richardson, M.O.W. Impact strength of composites with nano-enhanced resin after fire exposure. *Compos. Part B Eng.* **2014**, *56*, 290–295. [[CrossRef](#)]
24. Silva, S.P.; Sabino, M.A.; Fernandes, E.M.; Correló, V.M.; Boesel, L.F.; Reis, R.L. Cork: Properties, capabilities and applications. *Int. Mater. Rev.* **2005**, *50*, 345–365. [[CrossRef](#)]
25. Mano, J.F. The viscoelastic properties of cork. *J. Mater. Sci.* **2002**, *37*, 257–263. [[CrossRef](#)]
26. Rosa, M.E.; Fortes, M.A. Deformation and fracture of cork in tension. *J. Mater. Sci.* **1991**, *26*, 341–348. [[CrossRef](#)]
27. Reis, P.N.B.; Ferreira, J.A.M.; Silva, P.A.A. Mechanical behaviour of composites filled by agro-waste materials. *Fibers Polym.* **2011**, *12*, 240–246. [[CrossRef](#)]
28. Petit, S.; Bouvet, C.; Bergerot, A.; Barrau, J.J. Impact and compression after impact experimental study of a composite laminate with a cork thermal shield. *Compos. Sci. Technol.* **2007**, *67*, 3286–3299. [[CrossRef](#)]
29. Silva, F.G.A.; de Moura, M.F.S.F.; Magalhães, A.G. Low velocity impact behaviour of a hybrid carbon-epoxy/cork laminate. *Strain* **2017**, *53*, 1–9. [[CrossRef](#)]
30. Amaro, A.M.; Reis, P.N.B.; Ivañez, I.; Sánchez-Saez, S.; Garcia-Castillo, S.K.; Barbero, E. The High-velocity impact behaviour of Kevlar composite laminates filled with cork powder. *Appl. Sci.* **2020**, *10*, 6108. [[CrossRef](#)]
31. Reis, P.N.B.; Ferreira, J.A.M.; Costa, J.D.M.; Santos, M.J. Fatigue performance of Kevlar/epoxy composites with filled matrix by cork powder. *Fibers Polym.* **2012**, *13*, 1292–1299. [[CrossRef](#)]
32. Ivañez, I.; Sánchez-Saez, S.; Garcia-Castillo, S.K.; Barbero, E.; Amaro, A.; Reis, P.N.B. High-velocity impact behaviour of damaged sandwich plates with agglomerated cork core. *Compos. Struct.* **2020**, *248*, 112520. [[CrossRef](#)]
33. Gong, S.; Toh, S.; Shim, V. The elastic response of orthotropic laminated cylindrical shells to low-velocity impact. *Compos. Eng.* **1994**, *4*, 247–266. [[CrossRef](#)]
34. Krishnamurthy, K.; Mahajan, P.; Mittal, R. Impact response and damage in laminated composite cylindrical shells. *Compos. Structur.* **2003**, *59*, 15–36. [[CrossRef](#)]
35. Krishnamurthy, K.; Mahajan, P.; Mittal, R. A parametric study of the impact response and damage of laminated cylindrical composite shells. *Compos. Sci. Technol.* **2001**, *61*, 1655–1669. [[CrossRef](#)]
36. Kistler, L. Experimental investigation of the impact response of cylindrically curved laminated composite panels. In Proceedings of the 35th Structures, Structural Dynamics, and Materials Conference, Hilton Head, SC, USA, 18–20 April 1994; pp. 2292–2297, AIAA paper, 94-1604-CP. [[CrossRef](#)]
37. Kistler, L.S.; Waas, A.M. Experiment and analysis on the response of curved laminated composite panels subjected to low velocity impact. *Int. J. Impact Eng.* **1998**, *21*, 711–736. [[CrossRef](#)]
38. Zhao, G.; Cho, C. Damage initiation and propagation in composite shells subjected to impact. *Compos. Struct.* **2007**, *78*, 91–100. [[CrossRef](#)]
39. Kumar, S. Analysis of impact response and damage in laminated composite shell involving large deformation and material degradation. *J. Mech. Mater. Struct.* **2008**, *3*, 1741–1756. [[CrossRef](#)]
40. Arachchige, B.; Ghasemnejad, H.; Augousti, A.T. Theoretical approach to predict transverse impact response of variable-stiffness curved composite plates. *Compos. Part B Eng.* **2016**, *89*, 34–43. [[CrossRef](#)]
41. Arachchige, B.; Ghasemnejad, H. Post impact analysis of damaged variable-stiffness curved composite plates. *Compos. Struct.* **2017**, *166*, 12–21. [[CrossRef](#)]
42. Coelho, C.A.C.P.; Navalho, F.V.P.; Reis, P.N.B. Impact response of laminate cylindrical shells. *Frat. Integrita Strutt.* **2019**, *48*, 411–418. [[CrossRef](#)]
43. Amaro, A.M.; Reis, P.N.B.; Magalhães, A.; De Moura, M.F.S.F. The Influence of the Boundary Conditions on Low-Velocity Impact Composite Damage. *Strain* **2011**, *47*, e220–e226. [[CrossRef](#)]
44. Chaudhuri, R.A.; Hsia, R.L. Effect of thickness on the large elastic deformation behavior of laminated shells. *Compos. Struct.* **1998**, *43*, 117–128. [[CrossRef](#)]
45. Kimn, D.; Chaudhuri, R.A. Effect of Thickness on Buckling of Perfect Cross-Ply Rings under External Pressure. *Compos. Struct.* **2007**, *81*, 525–532. [[CrossRef](#)]
46. Chaudhuri, R.A. Effects of thickness and fibre misalignment on compression fracture in cross-ply (very) long cylindrical shells under external pressure. *Proc. R. Soc. A* **2015**, *471*, 20150147. [[CrossRef](#)]
47. Reis, P.N.B.; Ferreira, J.A.M.; Antunes, F.V.; Costa, J.D.M. Flexural behaviour of hybrid laminated composites. *Compos. Part A Appl. Sci. Manuf.* **2007**, *38*, 1612–1620. [[CrossRef](#)]
48. Silva, M.P.; Santos, P.; Sousa, N.N.; Reis, P.N.B. Strain rate effect on composites with epoxy matrix filled by cork powder. *Mater. Des. Process Comm.* **2019**, *1*, e47. [[CrossRef](#)]
49. Reis, P.N.B.; Silva, M.P.; Santos, P.; Parente, J.M.; Bezazi, A. Viscoelastic behaviour of composites with epoxy matrix filled by cork powder. *Compos. Struct.* **2020**, *234*, 111669. [[CrossRef](#)]
50. Reis, P.N.B.; Silva, M.P.; Santos, P.; Parente, J.M.; Valvez, S.; Bezazi, A. Mechanical performance of an optimized cork agglomerate core-glass fibre sandwich panel. *Compos. Struct.* **2020**, *245*, 112375. [[CrossRef](#)]
51. Oliveira, V.; Rosa, M.E.; Pereira, E. Variability of the compression properties of cork. *Wood Sci. Technol.* **2014**, *48*, 937–948. [[CrossRef](#)]
52. Silva, M.P.; Santos, P.; Parente, J.; Valvez, S.; Reis, P.N.B. Effect of harsh environmental conditions on the impact response of carbon composites with filled matrix by cork powder. *Appl. Sci.* **2021**, *11*, 7436. [[CrossRef](#)]

53. Giancaspro, J.W.; Papakonstantinou, C.G.; Balaguru, P.N. Flexural Response of Inorganic Hybrid Composites with E-Glass and Carbon Fibers. *J. Eng. Mater. Technol.* **2010**, *132*, 021005. [[CrossRef](#)]
54. Dong, C.S.; Duong, J.; Davies, I.J. Flexural properties of S-2 glass and TR30S carbon fiber reinforced epoxy hybrid composites. *Polym. Compos.* **2012**, *33*, 773–781. [[CrossRef](#)]
55. Dong, C.; Davies, I.J. Optimal design for the flexural behaviour of glass and carbon fibre reinforced polymer hybrid composites. *Mater. Des.* **2012**, *37*, 450–457. [[CrossRef](#)]
56. Schoeppner, G.A.; Abrate, S. Delamination threshold loads for low velocity impact on composite laminates. *Compos. Part A Appl. Sci.* **2000**, *31*, 903–915. [[CrossRef](#)]
57. Belingardi, G.; Vadori, R. Low velocity impact of laminate Glass-Fiber-Epoxy matrix composite materials plates. *Int. J. Impact. Eng.* **2002**, *27*, 213–229. [[CrossRef](#)]
58. Amaro, A.M.; Reis, P.N.B.; de Moura, M.; Santos, J.B. Influence of the specimen thickness on low velocity impact behavior of composites. *J. Polym. Eng.* **2012**, *32*, 53–58. [[CrossRef](#)]
59. Babu, M.G.; Velmurugan, R.; Gupta, N.K. Energy absorption and ballistic limit of targets struck by heavy projectile. *Lat. Am. J. Solids Struct.* **2006**, *3*, 21–39.
60. García-Castillo, S.K.; Sánchez-Sáez, S.; Barbero, E. Influence of areal density on the energy absorbed by thin composite plates subjected to high-velocity impacts. *J. Strain Anal.* **2012**, *47*, 444–452. [[CrossRef](#)]
61. Wen, H.M. Penetration and perforation of thick FRP laminates. *Compos. Sci. Technol.* **2001**, *61*, 1163–1172. [[CrossRef](#)]
62. Naik, N.K.; Shirao, P.; Reddy, B.C.K. Ballistic impact behavior of woven fabric composites: Parametric Studies. *Mater. Sci. Eng. A Struct. Mater. Prop. Microstruct. Process* **2005**, *412*, 104–116. [[CrossRef](#)]
63. Gama, B.A.; Gillespie, J.W. Punch shear based penetration model of ballistic impact of thick-section composites. *Compos. Struct.* **2008**, *86*, 356–369. [[CrossRef](#)]
64. Grujicic, M.; Glomski, P.S.; He, T.; Arakere, G.; Bell, W.C. Material modelling and ballistic-resistance analysis of armor-grade composites reinforced with high-performance fibers. *J. Mater. Eng. Perform.* **2009**, *18*, 1169–1182. [[CrossRef](#)]
65. Zhu, G.; Goldsmith, W.; Dharan, C.K.H. Penetration of laminated Kevlar by projectiles-II. Analytical model. *Int. J. Solids Struct.* **1992**, *29*, 421–436. [[CrossRef](#)]
66. He, T.; Wen, H.M.; Qin, Y. Penetration and perforation of FRP laminates struck transversely by conical-nosed projectiles. *Compos. Struct.* **2007**, *81*, 243–252. [[CrossRef](#)]
67. Fernandes, F.A.O.; Pascoal, R.J.S.; Alves de Sousa, R.J. Modelling impact response of agglomerated cork. *Mater. Des.* **2014**, *58*, 499–507. [[CrossRef](#)]